SHOCK PULSE GENERATION USING EXPLOSIVE DRIVEN METAL DRIVERS - PRACTICAL CONSIDERATIONS

G.M. WESTON, G.F. WHITTY AND E. NORTHEAST

MRL-TR-93-3

AUGUST 1993

MATERIALS RESEARCH LABORATORY

DSTO

Shock Pulse Generation Using Explosive-Driven Metal Drivers - Practical Considerations

G.M. Weston, G.F. Whitty and E. Northeast

MRL Technical Report
MRL-TR-93-3

Abstract

The present paper examines the practical aspects of using the mousetrap plane wave generator design to shock-harden metal targets of iron and copper. The paper investigates three driver plate designs and two plate sizes and compares the experimental x-ray plate profile with that provided by the modelling code Dyna 3D for the same run conditions. For the larger driver plate series of 110 mm square, the central planar area available for shock hardening using the full plate compared favourably with that provided by the driver design incorporating steel edge confinement. Drivers using explosive overhang as driver edge confinement provided the smallest central planar area for shock hardening. Shock hardening was not possible with smaller drives of 55 mm square due to the degree of plate curvature experienced before target impact. The modelling code Dyna 3D provided close agreement with experiment for the smaller driver series except where steel edge confinement was used, while for the larger driver series the modelling code consistently predicted greater plate curvature for all three designs than was experienced in practice.

DEPARTMENT OF DEFENCE
DSTO MATERIALS RESEARCH LABORATORY

Published by

DSTO Materials Research Laboratory
Cordite Avenue, Maribyrnong
Victoria, 3032 Australia

Telephone: (03) 246 8111
Fax: (03) 246 8999

AR No. 008-255

APPROVED FOR PUBLIC RELEASE

Authors

G.M. Weston

George Weston has worked at MRL since graduating from RMIT in 1970 obtaining a Diploma in Secondary Metallurgy. During this period he has been involved in several areas of research namely, solidification, secondary steel making, metal surfacing and while on secondment in the UK aspects of aircraft sabotage. Recent research has involved the interaction of materials and explosives within the Ship Structures and Materials Division.

G.F. Whitty

Fred Whitty commenced work at Materials Research Laboratory in 1947 as a Junior Laboratory Assistant. He qualified from Royal Melbourne Institute of Technology in 1955 and has worked as an Experimental Officer in several areas of defence science since that time. In recent years his areas of expertise have been concentrated on Terminal Ballistics, Flash x radiography, Industrial Radiography and Photometry.

E. Northeast

Eric Northeast graduated with a BSc in Computer Science/Physics in 1989 from Chisholm Institute of Technology. He joined MRL in 1982, where he worked in the areas of hydro-code modelling, slapper detonator fuze research and is currently managing computing in the Explosives Ordnance Division, MRL.

Contents

Shock Pulse Generation Using Explosive-Driven Metal Drivers - Practical Considerations

1. Introduction

The quantitative study of material behaviour under high strain-rate impulsive loading conditions, requires the capability to accurately reproduce planar shock pulse loading with the identical characteristics of the system under investigation. In the past the most common approach has been to generate planar shock waves using either a two-explosive, inert core lens system [1,2] or a flying plate generator which is often referred to as the mousetrap design [1-6].

The mousetrap design uses the ratio of the driven plate velocity to explosive detonation velocity to effect refraction within the target material. Although relatively simple in principle, this device is known to suffer from several inherent defects, the most notable being that the outer edges of the driver plate receive a shorter loading pulse than the plate centre. The resultant plate edge lag substantially reduces the available planar area of the original flyer plate. For high strain-rate shock hardening studies of metal samples, this available planar area governs the useable sample size. Precise manufacture of the mousetrap apparatus is also required to ensure reproducible plane wave conditions [1]. The two-explosive, plane wave initiating lens, although having the potential to provide greater accuracy, requires precision explosive pressing, casting or machining capability for manufacture; facilities which are not always readily available. When used to propel a plate, explosive lens systems also deliver a non-uniform pressure pulse again due to edge pressure losses, which results in curvature of the driving plate. [1].

To obviate the need for specialised explosive machining and casting facilities,the mousetrap plane wave generator design was chosen for shock hardening metal targets. The present paper reports on the implementation of this design to deliver a predetermined planar shock pulse for shock hardening of selected metal targets. To assist in driver plate design and optimisation, the Finite Element Analysis (FEA) code DYNA3D, was used to simulate driver edge profile formation for each driver plate configuration under consideration.

2. Experimental Theory

2.1 Assembly Design Considerations

The flying plate, plane wave generator assembly used for the shock-hardening study is illustrated in Figure 1. Essentially this is a two stage device. Firstly, detonation of the line wave initiator at the apex of the perforated triangular area is designed to provide a linear detonation front for initiation of the remaining unperforated section of the explosive/glass sandwich. The separation angle between the glass plane wave initiator and main flyer charge is calculated using the detonation velocity of the sheet explosive, to ensure that all the explosively driven glass particles arrive simultaneously at the driver plate explosive charge surface and thus guarantee planar initiation.

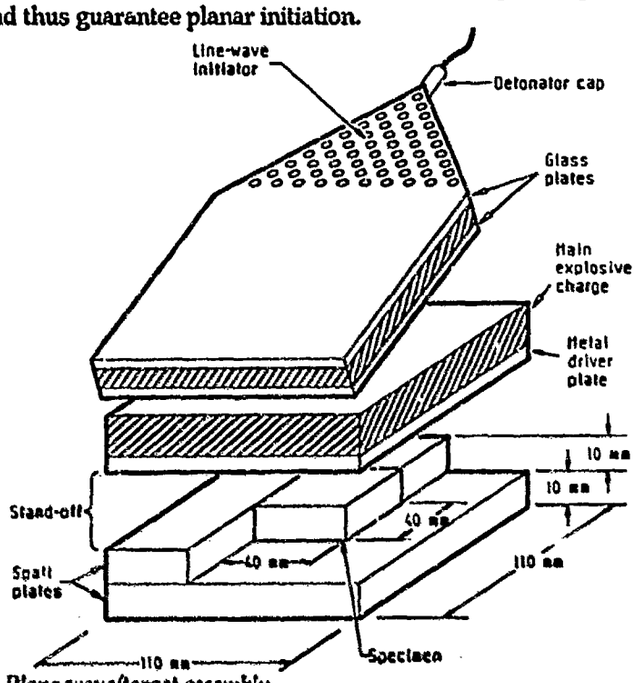

Figure 1: Plane wave/target assembly.

The uniform planar pressure pulse produced by the driver plate explosive is transferred to the driver plate and ensures that the driver plate front face remains parallel to the target surface, and on impact with the target delivers an essentially planar flat-topped compressive pressure pulse. The above operational sequence is shown schematically in Figure 2. In practice, however, the use of an unconfined charge, such as is used in this design, will result in the outer plate edge receiving a discernibly shorter driving shock pulse, the resultant plate edge lag loading to curvature of the plate surface during in-flight formation.

To ensure the target receives only a compressive shock pulse followed by an accompanying rarefaction, careful consideration must be given to both component material selection and target design and assembly. Identical materials or materials with closely matched Hugoniots must be used for both driver and target assembly components. The Hugoniots describe the physical properties of a material under shock loading (2). Correct materials selection guarantees a

uniform shock impedance and reduces the level of shock reflections normally experienced at acoustically dissimilar metal interfaces. Similarly, target assembly interfaces, between the target and abutting momentum traps and spall plate, must be closely mated to the target using accurate machining. This procedure reduces the magnitude of the secondary relief waves which are commonly experienced at free surfaces during the passage of a planar compressive wave.

The width of side momentum trap assembly components must also be sufficient to prevent tensile relief waves from exterior surfaces re-entering the target, and introducing secondary metallurgical damage or microstructural features uncharacteristic of a planar compressive wave. The base spall plate thickness should ensure that the incident compressive wave and accompanying rarefaction can pass into the spall plate before the reflected tensile wave from the back surface reaches the spall plate specimen interface. Rose and Grace in their work, provide mathematical models based on the mechanics of shock-wave propagation to assist in determining these values [6].

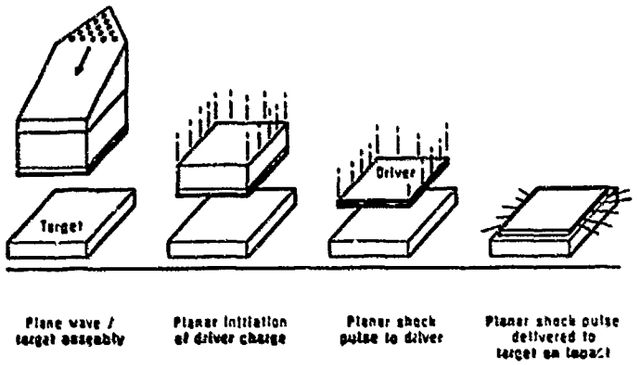

Figure 2: Sequence of plane wave generator operation.

2.2 *Driver Velocity Determination*

For the simple flyer plate system shown in Figure 1, a planar shock pulse of predetermined peak pressure and pulse duration can be delivered at the target surface by the manipulation of driver plate thickness and velocity. For a given peak pressure requirement, the particle velocity, U_p, within the target regime can be obtained directly for most metal and metal alloy systems from readily available Hugoniot data. As the driver plate velocity, U_d, is equal to the free surface velocity U_f of the target material $U_d = U_f$ for compressive shock pulse loading, the relationship between U_f and U_p in the target regime can be inferred from Equation 1.

$$U_f = 2U_p \qquad (1)$$

For the mousetrap assembly design, a close estimate of driver plate velocity for a given driver/charge combination is obtained using the Gurney relationship for an open faced sandwich situation (9) shown in Equation 2.

$$V_d = \frac{\sqrt{2E}\ \sqrt{3}\ C/M}{\left[(C/M+4)(C/M+1)\right]^{1/2}} \qquad (2)$$

Where V_d is the driver velocity, $\sqrt{2E}$ identifies the Gurney constant for the explosive, M denotes the metal mass and C the explosive mass. These latter two terms are obtained as a product of the thickness and density of the material in question. From equation 2, it can be seen that the pressure pulse delivered at the specimen surface is a function of the thickness and density of the driver material, and detonation velocity of explosive type used. Accordingly the driver velocity can be modified by simple design variations and the judicious selection of explosive. The actual driver plate velocity can, however, be more accurately determined during the experiment using flash x-ray imaging of plate movement..

Shock pulse duration D_t as expressed in equation 3 can again be simply adjusted by changing driver thickness h_d or explosive thickness.

$$D_t = \frac{2h_d}{U_s} \qquad (3)$$

where U_s represents the shock velocity for the particular material system under study and can be readily calculated from the Hugoniot relationship for the material system given U_p, or peak pressure requirement.

3. *Experimental*

The plane wave generator used in the present work was based on design details provided by Dupont in a technical bulletin (8). Although reference was made to the use of special glues for mousetrap construction, it was found that the assembly of all components including the attachment of the main driver charge and driver plate could be successfully achieved using masking tape.

Two driver assembly designs were used in this test program. Series A drivers consisted of 3 mm thick Remco iron plate 55 mm or 41 mm square with 7 mm wide steel confinement strips or 7 mm of explosive overhang extending around the outer driver edge. These configurations were designated A1, A2, and A3 respectively, Figure 3. This driver series was used with a standard charge size 55 mm square x 15 mm. Charge length includes 4mm thick layer of explosive associated with plane wave generator B series drivers consisted of 3 mm thick Remco iron plate 110 mm or 90 mm square with 10 mm wide steel confinement strips or 10 mm of explosive overhang extending around the outer driver plate edge and were designated B1, B2 and B3 respectively. The B series was used with a standard explosive charge size 110 mm square x 25 mm . Both driver series were designed to match the end dimensions of the respective charges, with or without steel edge confinement, or to allow an explosive overhang approximating half the explosive charge thickness, a formula which was based on the requirments specified by Walters [9]. For an unconfined driver charge, edge confinement based on the above formula was reported to ensure a more uniform

pressure gradient across the driver surface thereby reducing the amount of in-flight plate curvature.

Several high purity OFHC copper (Cu 99.999%) targets were also shock hardened. For copper, only B1 series drivers were used. The experimental procedure was identical to that used for iron, with the exceptions that driver thickness was reduced to 2.6 mm and explosive charge length reduced to 20 mm to provide similar shock pulse conditions to those used for the iron specimens.

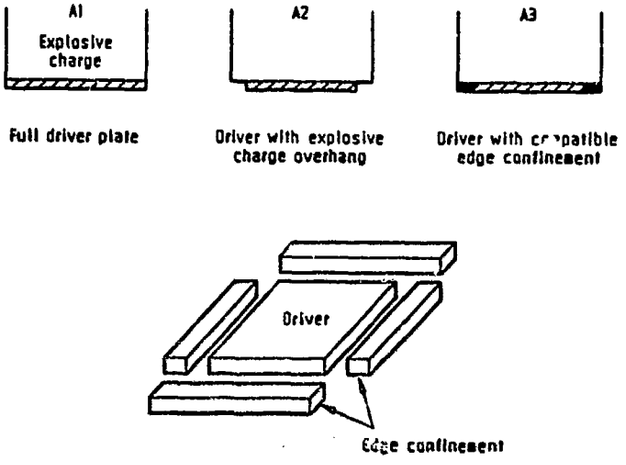

Figure 3: Driver configurations.

Driver explosive charges were built up from 2 mm thick Dow Corning DETTA sheet having an experimentally measured detonation velocity of 7216 m/s. In all instances, the main driver plate faces were machined parallel with a thickness tolerance of ±0.050 mm, an extremely close tolerance fit with the driver edge confinement strips was not required.

Target assembly details are provided in Figure 1, and follow established design concepts developed elsewhere [3, 5, 6]. The spall plates surrounding the central Remco iron target were machined from mild steel. This material has a closely matched Hugoniot to that of the target material to reduce shock reflections which occur at dissimilar metal interfaces. The possibility of shock reflections at assembly interfaces was further minimized by machining and then final grinding interfaces to achieve a micro surface finish of N4 and tolerance fit of ± 0.002 mm.

For shock hardening, the line wave and target assembly was situated above two vertically stacked plastic rubbish bins filled with water and separated by two layers of Cancite, Figure 4. The target assembly support platform consisted of a styrofoam base, 220 x 220 x 50 mm, attached using double sided tape to two 50 mm square styrofoam support bars aligned with the opposite edges of the base. Support bars were positioned across the upper rubbish bin rim so that the support base rested within the bin top.

The driver surface was aligned parallel with respect to the target assembly using an accurately machined spacer. Styrofoam supports in contact with the base platform were then attached using double sided tape to the sides of the plane wave generator assembly and the spacer block separating driver and target removed. If required, the water level was adjusted to ensure contact with the styrofoam base and assist in supporting the target and driver assembly. Water also provides for soft deceleration of the target following driver impact thus minimising secondary damage and providing a quench medium to ensure retension of the shocked target microstructure. The experimental assembly was adjusted to ensure the target impact surface was aligned parallel to the centre line of the flash x-ray heads.

To obtain high quality driver plate images without film or cassette damage, two orthogonally positioned, independently pulsed, 600 kVA flash x-ray units with a film cassette size 130 x 180 mm were used. Both the film and intensifying screens were sandwiched between two lead sheets, thickness 0.10 mm front and 0.125 mm back, to prevent back-scatter and were enclosed in a 180 x 230 mm high density polythene cassette casing with face plate thickness of 30 mm for film protection. Cassettes were positioned 300 mm from the target centre and protected with a 6 mm thick aluminium cover plate. Sharp images were obtained using a charge voltage of 20 kV and output voltage of 440 kV. Delay x-ray trigger times of 61 to 62.5 ms from firing pulse provided driver images 3 mm to 5 mm from the target surface for series B drivers for a 30 mm driver/target separation.

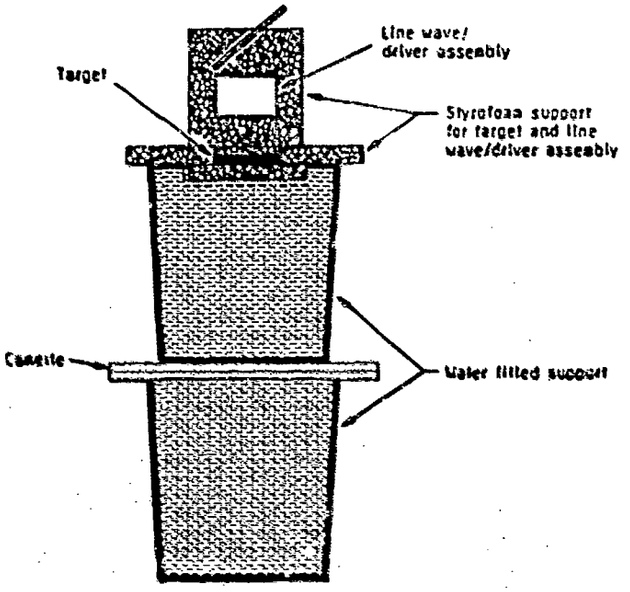

Figure 4: Experimental setup used for shock hardening.

Plate travel distance between the two sequentially pulsed x-ray images, was used to determine experimental velocity. X-ray trigger times were accurately recorded using a Hewlett Packard oscilloscope.

For all tests, planar impact was assumed if the projected driver/target impact angle was less than two degrees across the target surface (10).

The finite element modelling code Dyna3D, incorporating an elastic perfectly plastic material model, was used to provide a post detonation driver profile which could be used to assist experimental planning, and latter compared with the matching in-flight experimental images to confirm modelling code prediction accuracy.

The 40 mm experimental target dimension used was based on modelling code prediction for a series B2 driver to provide a 45 mm square central planar contact area, assuming a 30 mm target to driver separation.

4. Results and Discussion

4.1 Performance of Driver Assembly

During early testing the occurrence of non-planar driver impacts was found to be solely attributable to support platform instability. Static x-ray images of the driver and target setup before detonation, showed that flexing of the support platform could result in misalignment of target and driver surfaces, particularly after removal of the parallel sided alignment spacer. Where the styrofoam supports provided sufficient stiffness to the experimental assembly, planar impact with the target surface was consistently achieved using the plane wave generator of Dupont design.

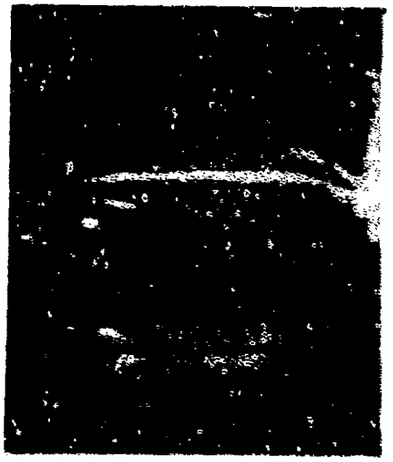

Figure 5: Driver X-ray Silhouette immediately before Target Impact.

For the series B drivers, a planar shock pulse condition was consistently achieved in the target material. The projected angle of driver/target contact was always less that one degree and often approached one half of a degree, well below the maximum two degrees allowable for the loss of plane wave conditions (10). A typical x-ray profile of a B1 series driver after 30 mm of travel and immediately before target impact is shown in Figure 5.

The use of styrofoam as a support material for the line wave/target assembly provided no significant impediment to x-ray imaging as well as limiting the secondary damage to x-ray cassettes. These advantages combined with manufacturing simplicity and short on-site set-up times far outweighed styrofoam's low strength disadvantage.

While the plane wave generator used in the present program was relatively easy to construct, care was required during the manufacture of the line wave initiator and in particular the accuracy of the explosive perforation dimensions. Relaxation and movement of the explosive material during cutting necessitated frequent hole reseizing to ensure dimensional accuracy before removal of the hole template. This particular problem is demonstrated in Figure 6 where slight variations in hole diameter were responsible for the non-linear detonation front shown in Figure 6a compared with the linear wave front achieved with accurately sized holes in Figure 6b.

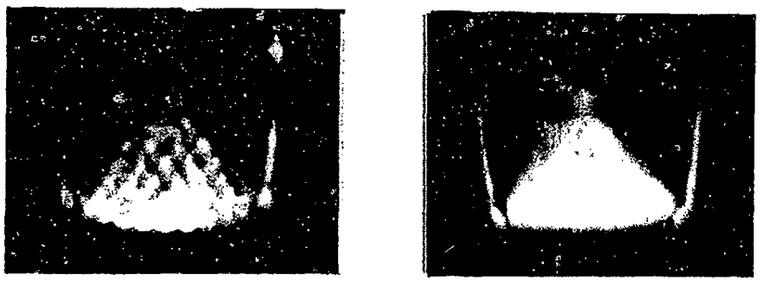

Figure 6: (a). Non-linear detonation front. *(b) Linear detonation front.*

4.2 Driver Distortion

For the smaller driver series, A1 to A3, the leading face of all driver plates showed severe curvature after only a few millimetres of travel, with edge confinement having only a marginal influence on the extent of final plate curvature, Figure 7. Given the level of plate curvature experienced with this driver series, realistic shock hardening experiments could not be contemplated.

For the larger driver series, B1 to B3, a central planar area of between 38 mm to 50 mm square was consistently achieved, given a 30 mm driver/target separation Figures 5&7. However, for any given driver type in this series, a small variation in the size of the central planar area of driver, available for shock-hardening, was observed between runs. From Figure 7, it is evident that steel edge confinement (series B2) was more effective than the equivalent distance of explosive overhang (series B3) in increasing the central area of plate available for shock hardening. Series B3 drivers also displayed greater plate edge thinning and spall. Drivers without steel edge confinement or explosive overhang (series B1) showed only slightly more plate curvature than series B2 plates (edge confinement) and consequently, provided an adequate central planar area for shock hardening. Although, both thinning and spall of the plate edge was more evident with the full plate than with the series B2 plates, a single full size driver in this size range provided a satisfactory result at significantly lower cost.

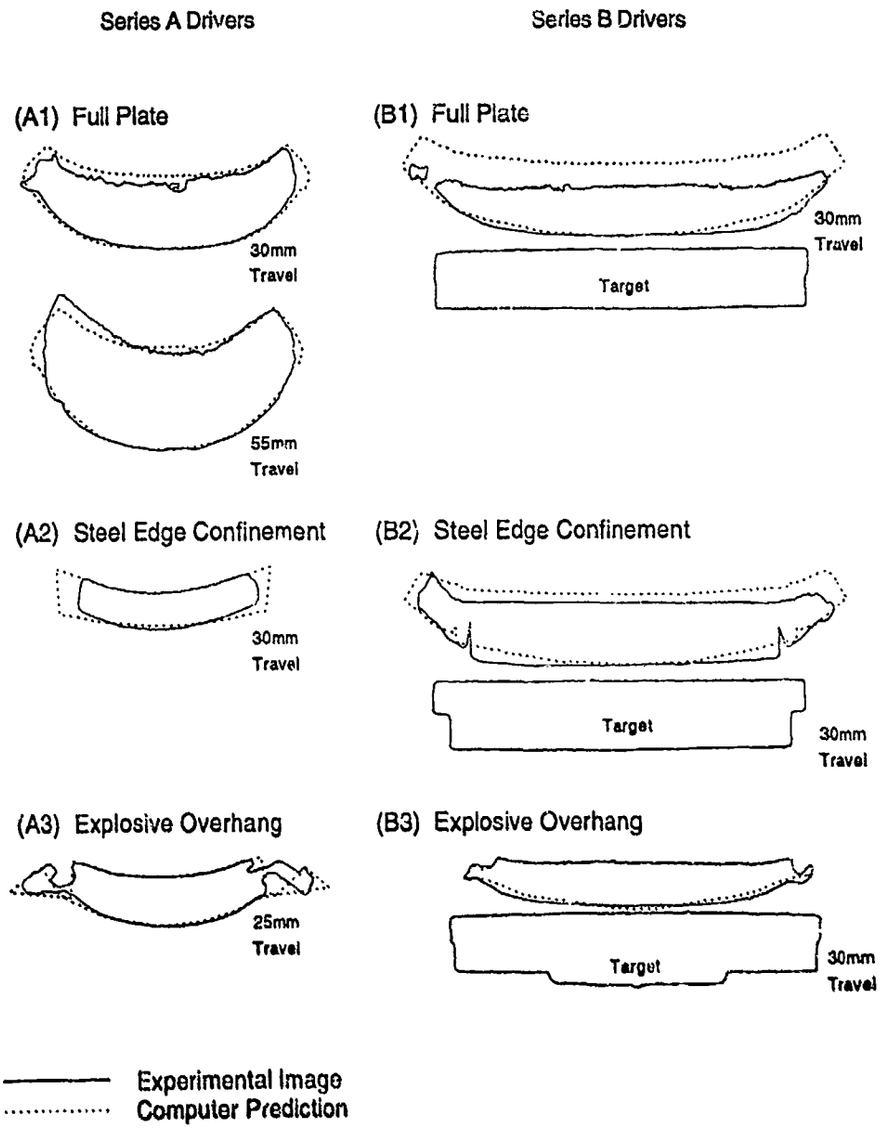
Series A Drivers
Series B Drivers
(A1) Full Plate
30mm
Travel
55mm
Travel
(B1) Full Plate
30mm
Travel
Target
(A2) Steel Edge Confinement
30mm
Travel
(B2) Steel Edge Confinement
Target
30mm
Travel
(A3) Explosive Overhang
25mm
Travel
(B3) Explosive Overhang
Target
30mm
Travel
Experimental Image
Computer Prediction

Figure 7:

For an unconfined explosive charge, the decrease in driver velocity, which accompanies edge pressure loss, can be estimated for any given plate size and charge thickness using Brown's method [7]. A plot of driver plate velocity versus plate size using this method for a constant explosive thickness of 20 mm is shown in Figure 8. This curve shows that a sharp decrease in plate velocity is predicted as driver plate dimensions are decreased below 100 mm. An increase in plate size above this value, however, results in only a small incremental increase in driver velocity. Given that it is the lower edge driving pulse that is responsible for the decrease in plate velocity, drivers in the size range of series A plates, could be expected to have a high pressure gradient across the plate surface and therefore experience considerable in-flight curvature as was observed in the present work. For the larger series B drivers, the influence of a smaller pressure gradient across the plate and steel edge confinement, provided a central planar area for shock hardening of between 45% to 50% that of the original plate area, for a driver/target separation of 30 mm.

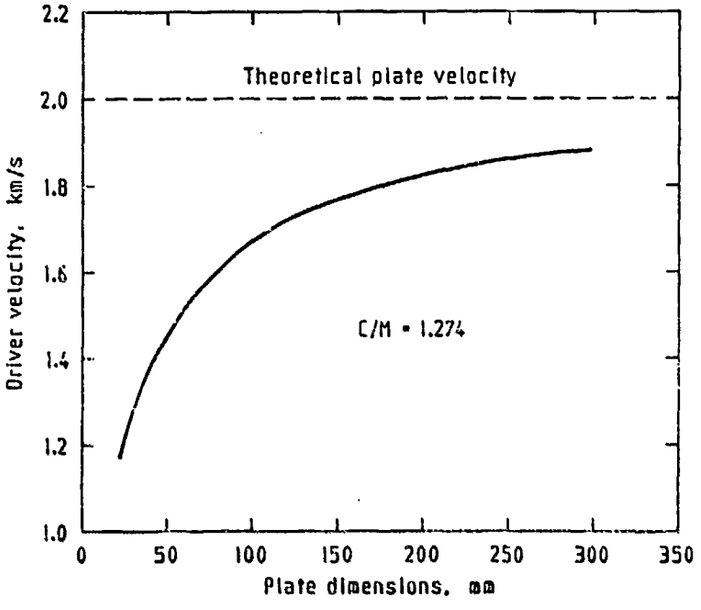

Figure 8: Relationship between driver size and final plate velocity for an confined charge condition.

4.3 *Target Examination*

Targets were recovered after shock hardening with only slight edge bruising and no visible surface fractures or defects. In all instances the measured reduction in the thickness of targets, following shock hardening, was typically less than 3%. A through thickness hardness traverse of shock hardened Remco iron targets, confirmed that uniform hardening had occurred. The base micro-hardness value for the as-received material was increased from 126 HV (100 g load) to 287 HV (100 g load). For copper targets, a uniform increase in the as-received hardness from 58 HV (100g load) to 157 HV (100g load) was recorded Figures 9a and 9b. The above hardness value for shocked Remco iron compares favourably with the

maximum plateau hardness value of 285 HV (100 g load) reported for a comparable iron and shock intensity [5].

Microstructural examination of hardened targets revealed no internal fractures and a uniform distribution of shock associated features throughout the microstructure. This suggests that the targets were subjected to a reasonably planar compressive shock pulse, and that the assembly design had prevented reflected tensile waves from exterior spall plate and momentum trap surfaces entering the target. It is considered an advantage to closely match spall plate to target thickness to ensure driver plate momentum is efficiently transferred through the target to the spall plate.

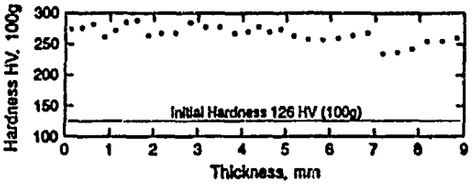

Figure 9 (a): Through-section hardness trace of a shocked Remco iron target.

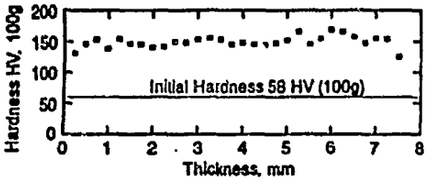

(b) Through-section hardness trace of a shocked copper target.

Examination of recovered spall plates always showed longitudinal fractures and reductions in thickness of approximately 50%. For iron, these spall fracture surfaces were smooth and substantially different to the coarser ductile fracture surfaces usually observed when the induced pressure did not exceed 130 Kbar [11].

4.4 Driver Velocity Determination

The cassette setup used provided sharp in-flight driver plate images for experimental velocity measurements without film damage Figure 5. The comparative results for driver velocities from direct measurement, calculations using the Gurney equation [7, 9] or provided by the modelling code Dyna3D are given in Table 1. For the larger drivers (series B1 to B3) this table shows excellent agreement to within 5% for all three methods. For the Gurney calculation, the 4 mm thick explosive layer positioned above the 3 mm thick glass sheet was included as part of the total charge for all calculations. Allowing for an estimated 5% error in the experimentally determined velocity value, both indirect methods provided a close estimate of final plate velocity. For the smaller drivers (series A1 to A3), the marked effect of edge pressure loss on final plate velocity, as illustrated in Figure 8, is apparent. The Gurney velocity estimate for this driver series is considerably higher than the experimentally determined value and this variation can be accounted for, using Brown's method [7], by the decrease in driver velocity due to edge pressure loss. Once edge pressure loss effects are included, both the experimental and calculated velocity values were within 8%. The modelling code plate velocity, however, appears not to have been affected by

edge pressure loss. With the larger drivers series, failure of the code to correct for plate size would not have greatly influenced the final velocity outcome.

Table 1: Experimental and Estimated Driver Velocity

DRIVER DETAILS	DRIVER VELOCITY KmS^{-1}		
DRIVER SERIES A	Experimental Values	Code Estimate	Gurney Estimate
A1 Full plate 55 mm square.	1.255	1440	1.488 (1.223)*
A2 Plate 41 mm square plus steel edge confinement to 55 mm square.	1.270		
A3 Plate 41 mm square plus explosive overhang to 55 mm square.	1.080	1400	(1.1301)
DRIVER SERIES B			
B1 Full plate 110 mm	2.02	2.020	2.028 (1.684)
B2 Plate 90 mm square plus steel edge confinement to 110 mm square.	2.01		
B3 Plate 90 mm square plus explosive overhang to 110 mm square.	1.980	1.980	1.918 (1.634)

*( ) Velocity Value corrected for edge Pressure loss using Brown's method.

4.5 *Code/Experiment Comparison*

Code simulation and experimental driver profile comparisons for an equivalent travel distance are shown for both driver series A and B in Figure 7. For the smaller driver series A1 to A3,' the code image for the full plate situation (series A1) showed good agreement with experiment up to 55 mm of travel at which point considerable plate curvature had occurred. Close code agreement with experiment was also observed for the A3 plate where explosive overhang was used in place of edge confinement. However, in this instance, the smaller travel distance of 25 mm minimised the degree of plate curvature. In contrast, the experimental image for the A2 driver, with steel edge confinement, showed the plate to have a more convex curvature than predicted by the code. This observation of the experimental image showing greater plate curvature than that predicted by the code, was inconsistent with the results shown in Figure 7 for all the larger series B plates. However, as only one experimental firing of an A2 plate was performed, the experimental plate deformation could not be confirmed. For

the larger driver series B1 to B3, irrespective of the initial driver setup, the code profile of the leading plate edge for a run distance of 30 mm consistently predicted more plate curvature than that observed in experiment. As small variations in the experimental driver leading edge profile were observed from run to run, the comparative code image provided a close indication to what could be expected in practice.

A number of modelling runs were performed using the ZeuS finite element code, utilising dynamic material properties obtained for Remco iron in the shock-hardened and as-received condition [12, 13]. These dynamic material properties show that the yield strength of implusively loaded iron is increased to 1000 MPa prior to plastic flow commencing. ZeuS finite element simulations of driver profile provided similar results to that shown in Figure 7 for Dyna 3D. An increase in plate hardness, due to shock hardening, is therefore unlikely to account for the observed differences in plate profile between code simulation and experiment.

5. *Summary*

The mouse trap plane wave generator design used in the present work proved easy to construct, with no specialised equipment required for its manufacture. The use of styrofoam and double sided tape as line wave and target assembly support materials, provided a cost effective method requiring minimal set up time for undertaking shock hardening experiments. Using the above plane wave device and series B drivers of 110 mm square, a planar shock pulse condition was readily achieved in the target material. In all instances, the angle of impact between driver and target never exceeded one degree, and in most instances was less than one half of a degree, well below the two degree allowable for planar contact. The use of steel edge confinement with series B drivers had only a marginal influence on the central planar area available for shock-hardening. With steel edge confinement, a central planar area of up to 50 mm square was available, to undertake shock hardening experiments, while this was reduced to between 38 to 45 mm square for a single full plate without confinement. The test design using explosive overhang as plate edge confinement, provided the smallest central planar area of plate available for shock hardening. Irrespective of the presence of edge confinement for the smaller series A drivers of 55 mm square, plate curvature was severe enough to prevented the use of this design for shock hardening experiments. Accordingly, to minimise plate curvature and provide a practicable central planar driver area for shock hardening, driver dimensions would need to approach 110 mm square.

The target assembly design, although demanding and costly to manufacture, provided shock hardened targets without secondary metallurgical damage. All examined targets showed both uniform hardening and regular distribution of microstructural shock features. The modelling code Dyna 3D provided close agreement for the smaller driver series except for the driver plate design with steel edge confinement. For the larger driver series however, the modelling code output for all three plate configurations, indicated greater curvature of the driver plate leading edge than were observed in experiment.

6. *References*

1. Duvall, G.E. and Fowlers, G R (1963). *High pressure physics and chemistry* (Vol 2), Ed. R.S. Bradley. New York: Academic Press.

2. Murr, Lawrence, E., and Staudhammer, Karl. P. (1988). *Shockwaves for industrial applications.* Ed. Lawerence E. Murr (Noyes Publications).

3. Dieter, G.E. (!958) *Responce of metal to high velocity deformation.* Eds P.G. Shewman and V.F.Zackay. London/New York: Interscience Publishers.

4. Rice, M. H., McQueen, R.G. and Walsh, J.H. (!958) *Advances in solid state physics* (Vol 6). Eds. Scity, F., and Turnbull, D. New York: Academic Press.

5. Smith, C. S. (1958). Metallographic studies of metals after explosive shock. *Trans. AIME,* 212, 574.

6. Rose, M. F. and Grace. F. I. (1967). A simple technique for shock deforming metal foils. *British Journal of Applied Physics.* 18, 671-674.

7. Crabtree, D. K. and Wagginen, S. S. (1987). *Gurney-type formulations for estimating initial fragment velocities for various warheads geometries* (NSWC TR 86-241).

8. Du Pont Chemical Products Sales Division-Explosives Department (1960). *Technical information on Du pont military specialties,* Bulletin No. ES-58-2A.

9. Walters, W.P. (1986). *Explosive loading of metals and related topics.* Special publication BRC-SP-56.

10. Belanger, C., Pelletier, P., and Drolet, J. F. (1958). Shock sensitivity study of curable plastic bonded explosives. *The Eighth Symposium (International) on Detonation,* 1, pp. 61-68. Albuquerque Convention Centre Albuquerque, New Mexico.

11. Banks, E. E. (1968). Fracture and fragmentation in shock loaded metals. *The Journal of the Australian Institute of Metals,* 13, 13-47.

SECURITY CLASSIFICATION OF THIS PAGE **UNCLASSIFIED**

REPORT NO.	AR NO.	REPORT SECURITY CLASSIFICATION
MRL-TR-93-3	AR-008-255	Unclassified

TITLE

Shock pulse generation using explosive-driven metal drivers - practical considerations

AUTHOR(S)
G.M. Weston, G.F. Whitty and
E. Northeast

CORPORATE AUTHOR
DSTO Materials Research Laboratory
PO Box 50
Ascot Vale Victoria 3032

REPORT DATE	TASK NO.	SPONSOR
August, 1993		

FILE NO.	REFERENCES	PAGES
G6/4/8-4460	11	21

CLASSIFICATION/LIMITATION REVIEW DATE

CLASSIFICATION/RELEASE AUTHORITY
Chief, Ship Structures and Materials Division

SECONDARY DISTRIBUTION

Approved for public release

ANNOUNCEMENT

Announcement of this report is unlimited

KEYWORDS

Planar Pressure Pulse
Compressive Shock Pulse
Driver Distortion
High Strain-Rate Impulsive Loading
Shock Hardening

ABSTRACT

The present paper examines the practical aspects of using the mousetrap plane wave generator design to shock-harden metal targets of iron and copper. The paper investigates three driver plate designs and two plate sizes and compares the experimental x-ray plate profile with that provided by the modelling code Dyna 3D for the same run conditions. For the larger driver plate series of 110 mm square, the central planar area available for shock hardening using the full plate compared favourably with that provided by the driver design incorporating steel edge confinement. Drivers using explosive overhang as driver edge confinement provided the smallest central planar area for shock hardening. Shock hardening was not possible with smaller drives of 55 mm square due to the degree of plate curvature experienced before target impact. The modelling code Dyna 3D provided close agreement with experiment for the smaller driver series except where steel edge confinement was used, while for the larger driver series the modelling code consistently predicted greater plate curvature for all three designs than was experienced in practice.

Shock Pulse Generation Using Explosive-Driven Metal Drivers
- Practical Considerations

G.M. Weston, G.F. Whitty and E. Northeast

(MRL-TR-93-3)

DISTRIBUTION LIST

Director, MRL
Chief, Ship Structures and Materials Division
Dr R.L. Woodward
Mr G.M. Weston
Mr G.F. Whitty
Mr E. Northeast
MRL Information Services

Chief Defence Scientist (for CDS, FASSP, ASSCM)	1 copy only
Director, Surveillance Research Laboratory	
Director (for Library), Aeronautical Research Laboratory	
Director, Electronics Research Laboratory	
Head, Information Centre, Defence Intelligence Organisation	
OIC Technical Reports Centre, Defence Central Library	
Officer in Charge, Document Exchange Centre	8 copies
Army Scientific Adviser, Russell Offices	
Air Force Scientific Adviser, Russell Offices	
Navy Scientific Adviser - data sheet only	
Scientific Adviser, Defence Central	
Director General Force Development (Land)	
Senior Librarian, Main Library DSTOS	
Librarian - MRL Sydney - data sheet only	
Librarian, H Block	
UK/USA/CAN/ABCA Armies Standardisation Rep., c/- DATD (NSO)	3 copies
Librarian, Australian Defence Force Academy	
Counsellor, Defence Science, Embassy of Australia - data sheet only	
Counsellor, Defence Science, Australian High Commission - data sheet only	
Scientific Adviser to DSTC Malaysia, c/- Defence Adviser - data sheet only	
Scientific Adviser to MRDC Thailand, c/- Defence Attache - data sheet only	
Head of Staff, British Defence Research and Supply Staff (Australia)	
NASA Senior Scientific Representative in Australia	
INSPEC: Acquisitions Section Institution of Electrical Engineers	
Head Librarian, Australian Nuclear Science and Technology Organisation	
Senior Librarian, Hargrave Library, Monash University	
Library - Exchange Desk, National Institute of Standards and Technology, US	
Exchange Section, British Library Document Supply Centre	
Periodicals Recording Section, Science Reference and Information Service, UK	
Library, Chemical Abstracts Reference Service	
Engineering Societies Library, US	
Documents Librarian, The Center for Research Libraries, US	